Cerebrospinal Fluid Proteome Changes in Older Non-Cardiac Surgical Patients with Postoperative Cognitive Dysfunction

Keith W. VanDusen[a], Yi-Ju Li[b,c], Victor Cai[a], Ashley Hall[a], Sarah Hiles[d], J. Will Thompson[d],
M. Arthur Moseley[d], Mary Cooter[a], Leah Acker[a], Jerrold H. Levy[a], Kamrouz Ghadimi[a],
Quintin J. Quiñones[a], Michael J. Devinney[a], Stacey Chung[a], Niccolò Terrando[a], Eugene W.
Moretti[a], Jeffrey N. Browndyke[f,g,h], Joseph P. Mathew[a] and Miles Berger[a,g,h,i,*] for the MADCO-PC
Investigators[1]

[a]*Department of Anesthesiology, Duke University Medical Center, Durham, NC, USA*
[b]*Department of Biostatistics and Bioinformatics, Duke University, Durham, NC, USA*
[c]*Duke Molecular Physiology Institute, Duke University, Durham, NC, USA*
[d]*Duke Center for Genomic and Computational Biology, Duke University, Durham, NC, USA*
[e]*Department of Neurology, Duke University Medical Center, Durham, NC, USA*
[f]*Department of Psychiatry & Behavioral Sciences, Division of Geriatric Behavioral Health, Duke University
Medical Center, Durham, NC, USA*
[g]*Duke Institute for Brain Sciences, Duke University, Durham, NC, USA*
[h]*Center for Cognitive Neuroscience, Duke University Medical Center, Durham, NC, USA*
[i]*Center for the Study of Aging and Human Development, Duke University Medical Center, Durham, NC, USA*

Abstract.

Background: Postoperative cognitive dysfunction (POCD), a syndrome of cognitive deficits occurring 1–12 months after surgery primarily in older patients, is associated with poor postoperative outcomes. POCD is hypothesized to result from neuroinflammation; however, the pathways involved remain unclear. Unbiased proteomic analyses have been used to identify neuroinflammatory pathways in multiple neurologic diseases and syndromes but have not yet been applied to POCD.

Objective: To utilize unbiased mass spectrometry-based proteomics to identify potential neuroinflammatory pathways underlying POCD.

Methods: Unbiased LC-MS/MS proteomics was performed on immunodepleted cerebrospinal fluid (CSF) samples obtained before, 24 hours after, and 6 weeks after major non-cardiac surgery in older adults who did ($n = 8$) or did not develop POCD ($n = 6$). Linear mixed models were used to select peptides and proteins with intensity differences for pathway analysis.

Results: Mass spectrometry quantified 8,258 peptides from 1,222 proteins in >50% of patient samples at all three time points. Twelve peptides from 11 proteins showed differences in expression over time between patients with versus without

*Correspondence to: Miles Berger, MD, PhD, Room 4317, Duke South Orange Zone, DUMC Box 3094, Durham, NC 27710, USA. Tel.: +1 919 684 8679; E-mail: miles.berger@duke.edu.; Twitter: @RealMilesBerger

POCD (q < 0.05), including proteins previously implicated in neurodegenerative disease pathophysiology. Additionally, 283 peptides from 182 proteins were identified with trend-level differences (q < 0.25) in expression over time between these groups. Among these, pathway analysis revealed that 50 were from 17 proteins mapping to complement and coagulation pathways (q = 2.44*10^{-13}).

Conclusion: These data demonstrate the feasibility of performing unbiased mass spectrometry on perioperative CSF samples to identify pathways associated with POCD. Additionally, they provide hypothesis-generating evidence for CSF complement and coagulation pathway changes in patients with POCD.

INTRODUCTION

Postoperative cognitive dysfunction (POCD) is a perioperative neurocognitive disorder often defined by a decrease of at least one standard deviation in measured cognitive function from baseline to 1–12 months after surgery. POCD, also referred to as neurocognitive disorder, postoperative when accompanied by subjective cognitive complaints or impaired ability to perform activities of daily living, occurs in up to 40% of older surgical patients [1–3] and is associated with decreased postoperative quality of life [4, 5], poor long-term cognitive outcomes [6], and elevated 1-year mortality [7]. With an aging population and over 16 million patients undergoing surgery each year in the U.S., POCD and other perioperative neurocognitive disorders constitute a growing public health concern [8].

Currently, prevention and treatment of POCD and other perioperative neurocognitive disorders remain limited by our incomplete understanding of their underlying mechanisms. These conditions are hypothesized to result from dysregulated immunity, including postoperative neuroinflammation, partly because neuroinflammation has been associated with cognitive deficits in preclinical models and several other neurocognitive disorders including Alzheimer's disease (AD) (reviewed) [9], multiple sclerosis [10, 11], and autoimmune encephalitis [11]. Indeed, patients with POCD exhibit elevated cerebrospinal fluid (CSF) inflammatory cytokines [12–14], microglial activation [15], blood-brain barrier dysfunction [16], and exacerbation of pre-existing AD-related pathology [14, 17, 18]. Many POCD biomarker studies have utilized targeted assays measuring specific proteins and inflammatory markers in blood and/or CSF samples before and after surgery [18–22]. However, these targeted assays limit investigation to pre-specified proteins of interest and lack the ability to identify novel proteins or pathways that may be involved in POCD.

In contrast to targeted assays, mass spectrometry-based approaches offer proteome-wide characterization by comparing peptide fragment intensities after a proteolytic preparation step. These intensities provide relative concentration measurements for thousands of peptide analytes, which are subsequently matched to their parent proteins. Mass spectrometry-based proteomics has the ability to identify novel protein targets and pathways underlying disease states in a hypothesis-independent, "unbiased" manner. Additionally, it can identify specific post-translational modifications, such as phosphorylation, that may be used to assess protein activation and signal cascade involvement [23].

Unbiased proteomic analyses have previously been used to identify novel biomarkers for mild cognitive impairment [24], AD [24–26], frontotemporal dementia [27, 28], Parkinson's disease [29], amyotrophic lateral sclerosis [28], HIV-related cognitive impairment [30], amygdala dysfunction [31], and chronic traumatic encephalopathy [32]. Recently, these methods have also been applied to postoperative delirium, revealing several preoperative CSF candidate biomarkers of postoperative delirium. Yet, to our knowledge, no other study has utilized unbiased mass spectrometry-based proteomics to identify novel CSF protein biomarker or pathway changes *after surgery* in older adults with perioperative neurocognitive disorders. In this pilot study, we examined the feasibility of using this approach to measure changes in CSF protein levels from patients with POCD compared to healthy controls in order to identify pathways that may contribute to POCD pathogenesis for further investigation in larger future studies

METHODS

Overview and patient selection

The protocol for this case-control study was approved by the Duke University Medical Center

Institutional Review Board as part of a parent observational cohort study registered with clinicaltrials.gov (NCT01993836) on November 25, 2013. All methods were carried out in accordance with relevant guidelines and regulations. All subjects gave written informed consent. For the parent study, we enrolled 140 English-speaking patients age 60 and above who were undergoing non-cardiac, non-neurologic surgery scheduled for at least 2 h under general anesthesia. All patients received propofol for anesthetic induction and either propofol or isoflurane for anesthetic maintenance. There were no exclusions for preoperative cognitive status; however, all patients had to be able to complete our cognitive test battery.

Cognitive testing

All patients included in the parent study underwent neurocognitive assessment at baseline and 6 weeks after surgery using our established neurocognitive test battery [6, 33–35] including the Randt Short Story Test, the Wechsler Memory Scale Modified Visual Reproduction Test, the Digit Span and Digit Symbol tests from the Revised Wechsler Adult Intelligence Scale, and the Trail Making Test, Part B. The scores from these tests were reduced to uncorrelated factor scores by factor analysis with orthogonal rotation, which were derived in a previous study of similar non-cardiac surgical patients [36]. This approach derived four factor scores that correspond to four cognitive domains: verbal memory; abstraction and visuospatial orientation; visual memory; and attention and concentration. Postoperative cognitive dysfunction was defined as a ≥ 1 standard deviation decrease in one or more of these four cognitive domain from baseline to 6 weeks after surgery as previously described [6, 34, 35, 37–42]. The 6-week time point was selected because it falls within the 1–12-month window that POCD/neurocognitive disorder, postoperative occurs, and the 6-week time point has been previously been used extensively in prior studies [6, 34, 35, 37–42]. Continuous Cognitive Index (CCI) scores were subsequently calculated for each patient by averaging their cognitive scores across all four domains and mean normalizing the results to zero. Thus, the CCI represents a single global measurement of cognitive function, with a positive score indicating above average overall cognitive testing performance and a negative score indicating below average performance compared to the reference study population [36].

Patient selection for proteomic analyses

From the patients in the parent MADCO-PC study, eight subjects with POCD, defined by a > 1 standard deviation decrease in at least one of four cognitive domains from before to six weeks after surgery, and six subjects without POCD at six weeks after surgery were selected for inclusion in this proteomics study. Prior work has questioned this definition of POCD because patients with a > 1 SD drop in one cognitive domain may nonetheless have a > 1 SD increase in another cognitive domain [43], calling into doubt whether such patients should really be considered to have cognitive dysfunction. Thus, to ensure that patients selected with POCD did have a true overall drop in cognition, and that those without POCD truly did not have even a minor overall drop in cognition (such as a < 1 SD drop in cognition across multiple domains), we added an additional constraint for selecting samples for each group. For the POCD group, we selected patients who had an overall drop in their continuous cognitive index (the mean of the four cognitive domain scores) from before to 6 weeks after surgery, in addition to a > 1 standard deviation decrease in at least one of four cognitive domains from before to six weeks after surgery. Likewise, for the non-POCD group, we selected patients who had an overall improvement in their continuous cognitive index from before to six weeks after surgery (perhaps reflective of a normal learning effect upon retesting), in addition to no drop of > 1 SD in any single cognitive domain over this time period. We prioritized selection

Table 1
Patient Characteristics

Characteristic	POCD	Non-POCD	Statistics
Number of patients	8	6	–
Age	71.25 ± 7.07	70.5 ± 5.75	$p = 0.836$
Percent Female	50%	33%	–
Years of Education	16 ± 4.34	16 ± 2.19	$p = 1.000$
Baseline CCI	0.100 ± 0.678	-0.010 ± 0.451	$p = 0.738$
CCI change at 6 weeks	-0.147 ± 0.215	0.173 ± 0.187	$p = 0.013$
APOE Genotypes Represented	*APOE ε3/3* (7) *APOE ε2/3* (1)	*APOE ε3/4* (2) *APOE ε3/3* (3) *APOE ε2/3* (1)	$p = 0.385$

Patient characteristics for the POCD and non-POCD groups. Values are presented as mean $\pm$ standard deviation, with p-values where appropriate. There were no significant differences in age, years of education, baseline CCI, CCI change at six weeks, or *APOE* genotype distribution between POCD and non-POCD groups. *P*-values for age, years of education, baseline CCI, and CCI change at six weeks calculated with two-tailed *t*-tests. *p*-value for *APOE* genotypes calculated using a Fisher's exact test.

of patients with similar age and years of education for both groups to avoid potential confounding from these factors (Table 1).

CSF and blood sample collection

Participants underwent baseline CSF and blood sampling within a month prior to surgery. Repeat CSF samples were obtained 24 ± 2 h after the start of surgery and 6 ± 3 weeks after surgery [33, 44]. CSF was collected using our protocol for minimizing pain and adverse events associated with lumbar puncture [40, 45]. Briefly, participants' lower backs were scrubbed with sterile iodine, and 20% benzocaine was applied by spray canister. After waiting 10 min for the local anesthetic to take effect, up to 5 mL of 1% lidocaine was injected subcutaneously at the targeted lumbar interspace. Subsequently, a 25-gauge spinal needle was inserted through 20-gauge introducers at the same interspace to extract approximately 10 mL of CSF using aseptic techniques. The puncture site was then covered with a bandage, and the patient was instructed to remain supine for at least 30 min to minimize the risk of post-dural puncture headache [45].

CSF and blood sample processing

CSF and blood supernatant aliquots were stored at –80°C, and initial blood samples were used for *APOE* genotyping by the Duke University DNA Analysis Facility (Durham, NC) using Applied Biosystems TaqMan SNP genotyping assays (10 ng DNA/assay) and an Applied Biosystems 7500 Fast Real-Time PCR system.

CSF samples (n = 42; one collected from each patient at each time point) were delivered to the Duke Proteomics and Metabolomics Shared Resource on dry ice, and gently thawed on ice. Coomassie Plus Bradford assays (Thermo Fisher Scientific, Waltham, MA, USA) were performed to determine protein concentrations, which varied from less than 0.125 μg/μL to greater than 2 μg/μL. 20 μL of human plasma was mixed with 730 μL of Sample Dilution Buffer (Agilent Technologies, Santa Clara, CA, USA) as a CSF-mimic positive control. For experimental samples, 600 μL of human CSF was mixed with 150 μL High Concentration Buffer (Agilent), such that the total volume for all samples (positive control and experimental samples was 750 μL. The diluted samples were then centrifuged through a 0.22 μm cellulose acetate centrifugal spin filter unit (Agilent) for 3 min at 15,000 rpm and 4°C. The filtered samples were transferred to Maximum Recovery LC glass v-bottom vials (Waters Corporation, Milford, MA, USA). 725 μL of each sample was immunodepleted to remove the high abundance plasma proteins using a MARS-14 LC column (Agilent) and an Agilent 1100 HPLC according to the manufacturer's protocol.

Following immunodepletion, samples were buffer exchanged with 50 mM ammonium bicarbonate using Amicon 10 MWCO (EMD Millipore, Burlington, MA, USA). Immunodepletion was quality-control checked by analysis of pre-versus post depletion samples on 4–13% Bis-Tris NuPAGE gel (Thermo) in MES buffer, and a Bradford protein assay of pre-versus post-depletion samples to confirm protein removal was consistent; protein removal via immunodepletion was on average 88.5%. Samples were then normalized to 8 μg each and supplemented to 0.1% w/v Rapigest detergent (Waters) for digestion. Samples were reduced with 10 mM dithiothreitol for 10 min at 80°C, alkylated with 20 mM iodoacetamide at room temperature in the dark for 30 min, and digested with 1:50 trypsin:protein (Promega Sequencing Grade) overnight at 37°C. After digestion, samples were acidified to 1/2/97 v/v/v TFA/MeCN/water and heated at 60°C for 1 h to hydrolyze Rapigest. 1 pmol ADH1_YEAST MassPrep standard (Waters) was added to each sample as a surrogate standard. Finally, a study pool QC (SPQC) sample was made by combining 5 μL of each digested sample.

Quantitative analysis of CSF proteins

Quantitative one-dimensional LC-MS/MS was performed on 2 μL (500 ng) of the protein digest per sample from all subjects in singlicate, with replicate analyses of the SPQC interspersed throughout at even intervals. Samples were analyzed using a nanoAcquity UPLC system (Waters) coupled to a Q Exactive Plus Orbitrap high resolution accurate mass tandem mass spectrometer (Thermo) via a nanoelectrospray ionization source. Briefly, the sample was first trapped on a Symmetry C18 300 mm × 180 mm trapping column (5 μL/min at 99.9/0.1 v/v H2O/MeCN), after which the analytical separation was performed using a 1.7 μm Acquity HSS T3 C18 75 mm × 250 mm column (Waters) using a 90 min gradient of 5 to 40% MeCN with 0.1% formic acid at a flow rate of 400 nL/min with a column temperature of 55°C. Data collection on the Q Exactive Plus mass spectrometer was performed in a data-dependent MS/MS manner, using a 70,000-resolution

precursor ion (MS1) scan followed by MS/MS (MS2) of the top 10 most abundant ions at 17,500 resolution. MS1 was accomplished using AGC target of $1*10^6$ ions and max accumulation of 60 msec. MS2 used AGC target of $5*10^4$ ions, 60 ms max accumulation, 2.0 m/z isolation window, 27 V normalized collision energy, and 20 s dynamic exclusion. The total analysis cycle time for each sample injection was approximately 2 h, and the experiment totaled 51 injections.

Samples were run in a randomized block design, and the QC Digest Pool was analyzed after every 6th sample within the group as well as at the beginning and end of the study. Following the analyses, the data was imported into Rosetta Elucidator v4.0 (Rosetta Biosoftware, Inc., Seattle, WA, USA), and all LC-MS files were aligned based on the accurate mass and retention time of detected ions ("features") using Rosetta Elucidator PeakTeller algorithm. The relative peptide abundance was calculated based on area-under-the-curve of aligned features across all runs. The dataset had 67,076 quantified features and HCD fragmentation was performed to generate approximately 1.62 M MS/MS spectra for sequencing by database searching.

Peptide identification and inclusion

The MS/MS data was searched against the UNI PROT protein sequence database with *Homo sapiens* species taxonomy, which also contained several surrogate standards sequences and common laboratory contamination proteins, as well as a reversed sequence "decoy" database for false discovery rate determination. Amino acid modifications allowed in database searching included fixed deamidation on Asn and Gln (*), carbamidomethyl Cys (**), and oxidation on Met (***). The data was searched with 5 ppm precursor, 0.02 Da product ion tolerance, and tryptic enzyme specificity, allowing up to two missed cleavages. Data was processed to the peptideTeller data curation algorithm to determine false discovery rate and was annotated at 0.5% peptide false discovery rate.

The raw peptide intensities were then scaled across all samples using robust mean scaling. To detect outliers, principal component analysis was performed for the scaled peptide intensities. By comparing principal components 1 and 2, one sample was found outside the cluster of the rest of samples. Therefore, this sample was excluded as an outlier. Additionally, two samples were processed in duplicate to ensure

agreement; peptide intensities from these samples were averaged for analysis. Peptide intensities that were missing (i.e., below the lower limit of detection) or below the 5th percentile of the non-missing intensities of each peptide were imputed with the 5th percentile of the non-missing intensities of that same peptide. Peptides that required imputation in more than 10 samples were excluded. To remove unstable peptides or those with poor precision, peptides with greater than 40% coefficient of variation across the QC pool were also excluded. Finally, the intensities of all the peptides and proteins were log2 transformed before statistical analysis.

Statistical analysis

Descriptive statistics were computed for key demographic and patient characteristics variables including age, sex, years of education, cognitive measures, and *APOE* genotypes by frequency (percentage) for categorical variable and mean (standard deviation, SD) for continuous variables. Two sample *t*-tests and Wilcoxon rank sum tests were conducted to compare the log2 transformed intensity difference of each peptide and protein between subjects who did and who did not have POCD at each time point (baseline, 24 h post-operation, and 6 weeks post-operation. To correct for multiple testing, q-values were computed for each peptide and protein at each time point [46]. Finally, to detect POCD effect on peptide intensity over time, linear mixed models were fitted for intensities of each peptide regressed on the fixed effects of group (i.e., POCD versus no POCD) from 24 h and 6 weeks after surgery, time, and interaction of group and time with random intercept and slope of time. Again, q-values of POCD effect were computed for each peptide and protein to correct for multiple testing. Proteins containing peptides meeting q < 0.25 were considered as candidates with probable POCD association.

Pathway analysis

Pathway analysis was conducted using the Database for Annotation, Visualization and Integrated Discovery with the Kyoto Encyclopedia of Genes and Genomes pathway database. This pathway analysis was performed on genes encoding proteins that contained top candidate peptides (q < 0.25) selected from our linear mixed model (described above). Significant pathways were determined by Benjamini-Hochberg false discovery rates (FDR) less than 0.05 (q < 0.05) from the pathway analysis [47].

RESULTS

Patient characteristics

Of the 14 patients included in the study, 8 developed POCD at 6 weeks after surgery, while 6 did not. Baseline/preoperative patient characteristics are listed in Table 1. The two groups were generally similar; there was no significant difference in age, years of education, baseline cognitive index, or *APOE* genotype distribution between groups ($p > 0.35$ for all). CCI change from before to 6 weeks after surgery was worse in the POCD group than the non-POCD group, as expected (–0.147 versus 0.173, $p = 0.013$).

CSF proteome characterization

Initial CSF analysis identified 8258 peptides that mapped to 1,222 proteins. 11 peptides were removed because they required imputation in 10 or more samples, and a small fraction (8.5%) of peptides were removed due to > 40% variability in the SPQC replicates across the course of the study. Therefore, the final quantitative dataset consisted of 7,542 peptides and 1,180 proteins for statistical analysis (Supplementary Material). No peptides from any of the three time points were found to be significantly different between the two groups after accounting for multiple testing with a threshold of $q < 0.05$, an unsurprising finding given the large number of peptides measured and small sample size.

Repeated measures and pathway analyses

Our linear mixed model analysis on peptide intensity over time did not detect any peptides that showed a statistically significant interaction of group by time at 24 h post-surgery but identified 12 peptides from 11 different proteins with statistically significant differences after FDR adjustment ($q < 0.05$) for the interaction term of group by time at 6 weeks post-surgery (Supplementary Table 1). Here, pre-surgery time was the reference. The 12 significant peptides accounted for approximately 7.3% of the 165 total peptides identified from those 11 proteins and included two different peptides from the copper carrying protein ceruloplasmin. Because our pilot study may have been underpowered to detect differences in other peptides, proteins, and pathways within a mixed model, we also examined peptides with q-values < 0.25 as previously described [48]. There were 283 unique peptides with $q < 0.25$ in these linear mixed models, which mapped to 182 unique parent proteins (Supplementary Table 1). These 283 peptides accounted for approximately 10.5% of the 2,694 total peptides identified derived from these 182 unique proteins.

To identify pathways that may be involved in the pathogenesis of POCD, the genes coding for these 182 proteins were mapped to functional pathways using the Kyoto Encyclopedia of Genes and Genomes pathway database (Table 2), and pathway analysis was conducted using the Database for Annotation, Visualization, and Discovery [49, 50]. This led to identification of nine pathways statistically associated at $p < 0.05$ with subsets of the 182 featured proteins (Supplementary Table 1). False discovery rates were also calculated for these pathways to account for type-1 error due to multiple comparisons. Kyoto Encyclopedia of Genes and Genomes pathway hsa 04610: Complement and coagulation cascades was found to be the most highly associated pathway, containing 50 of the total 283 peptides. These 50 peptides mapped to 17 different proteins (false discovery rate = 2.44×10^{-13}; Table 3). Finally, functional analysis was repeated using only the 12 peptides significant

Table 2
Functional pathway associations

Kyoto Encyclopedia of Genes and Genomes Pathway	Protein Count	p	False Discovery Rate
hsa04610: Complement and coagulation cascades	17	1.82×10^{-16}	2.442×10^{-13}
hsa05020: Prion diseases	8	1.63×10^{-07}	1.835×10^{-04}
hsa05150: Staphylococcus aureus infection	9	3.85×10^{-07}	4.328×10^{-04}
hsa04514: Cell adhesion molecules (CAMs)	11	1.38×10^{-05}	0.015
hsa04142: Lysosome	9	1.64×10^{-04}	0.183
hsa04512: ECM-receptor interaction	6	0.0054	5.836
hsa05322: Systemic lupus erythematosus	7	0.008	8.419
hsa05133: Pertussis	5	0.016	16.723
hsa00511: Other glycan degradation	3	0.022	22.428

A list of Kyoto Encyclopedia of Genes and Genomes pathways associated with subsets of the 182 proteins that contained significant peptides in our analysis.

Table 3
Peptides with q < 0.25 for time-group interaction at six weeks in the linear mixed model

Protein Name	Number of Peptides with q < 0.25
Complement C5	11
Plasma protease C1 inhibitor	1
Complement C3	1
Complement C2	2
Complement factor B	8
Kininogen 1	1
Complement C6	5
Complement C8b	3
Plasminogen	6
Complement C1s subunit	1
Complement factor H	1
Antithrombin-III	2
Complement C9	1
Coagulation factor 5	3
Complement Factor I	2
Fibrinogen	1
Prekallikrein	1

Proteins in the Kyoto Encyclopedia of Genes and Genomes pathway hsa04610: Complement and coagulation cascades pathway with q < 0.25 for time-group interaction in the linear mixed models.

at q < 0.05 rather than q < 0.25 (Supplementary Table 1) to assess whether they alone contributed to any known pathway; however, this did not reveal any significant pathway association.

To further study the role of complement in the pathogenesis of perioperative neurocognitive disorders, complement proteins with peptides that had trend-level significance (q < 0.25) in the linear mixed model (factors C1, C1s, C2, C3, C5, C6, C8b, C9, B, H, and plasma protease C1 inhibitor) were examined further. Though none of the individual peptides or proteins showed a statistically significant difference in intensity between the POCD and non-POCD groups at any single time point, trends in complement peptide and protein intensities were revealed (Figs. 1 and 2, Supplementary Figures 1–9). Notably, even with high peptide intensity variance across each group, the mean preoperative intensities for all complement peptides were consistently lower in patients who developed POCD than those who did not. Despite no significant differences between groups at this timepoint for any individual peptide, the probability of all 36 complement and related peptides randomly exhibiting this trend would be 0.5^{36}, or $1.455*10^{-11}$. When clustered by protein, the probability of this pattern occurring in the 12 complement proteins by chance would be 0.5^{12}, or $2.441*10^{-4}$.

Additionally, the patients who developed POCD exhibited overall rising trends in all complement proteins except complement factor H from baseline to

6-week time points, while patients without POCD exhibited decreasing intensity trends across the entire set of complement proteins over this time frame. For example, complement C5 was found to have 11 peptides approaching significance (q < 0.25) in our linear mixed model (Fig. 1A-L), with similar trends for peptides from both its alpha and beta subunits. Likewise, the five peptides from complement C6 (Fig. 2A-F), three peptides from complement C8b (Fig. 3A-D), and six of the eight peptides from complement factor B (Fig. 4A,B-I) with q < 0.25 were found to have similar patterns of convergence across the three time points between patients with and without POCD. Peptides from complement C2 (Supplementary Figure 1A-C), factor 1 (Supplementary Figure 2A-C), C1s, C3, C9, and plasma protease C1 inhibitor (Supplementary Figure 3A-J) also had similar trends. Among the non-complement proteins in this pathway with trend-level significance at q < 0.25, fibrinogen (Supplementary Figure 4A, B), antithrombin-III (Supplementary Figure 5A-C), and kallikrein (Supplementary Figure 6A, B) exhibited this convergence pattern, while kininogen-1 (Supplementary Figure 7A, B), plasminogen (Supplementary Figure 8A-G), and coagulation factor V (Supplementary Figure 9A-D) did not.

DISCUSSION

This pilot study represents one of the first unbiased proteomic analyses on pre- and postoperative CSF samples from older surgical patients with versus without perioperative neurocognitive disorders. We identified peptides from 11 proteins with statistically significant intensity changes (q < 0.05) between patients with versus without POCD in our FDR-adjusted linear mixed model. Pathway analysis revealed trend-level differences in 50 peptides from 17 complement and coagulation-related factors, suggesting a possible role for these pathways in POCD pathogenesis. Since we planned this study to evaluate the CSF proteome without focusing specifically on either these 11 proteins or the complement pathway, our findings illustrate the strength of unbiased CSF proteomic analyses for identifying potentially novel pathways in the pathogenesis of perioperative neurocognitive disorders. Additionally, our findings on the variability of CSF peptide levels in older surgical patients may prove useful for guiding power calculations when planning future studies.

We identified 12 peptides from 11 proteins that satisfied the stringent significance threshold of $q < 0.05$ (Supplementary Table 1) in our linear mixed model examining an interaction between groups (POCD versus no POCD) and postoperative time points. Several of these 11 proteins have been previously implicated in other neurocognitive disorders. First, cystatin C appears to play a neuroprotective role in AD, possibly through inhibition of cerebral amyloidosis [51, 52]. Furthermore, low cystatin C levels and certain cystatin C polymorphisms have been identified as predisposing factors to AD (reviewed) [53] and contribute to poor cognitive outcomes in Parkinson's disease [54], after ischemic strokes [55], and in HIV-associated neurocognitive disorder [56]. Similarly, multiple peptides representing the copper and iron-handling protein ceruloplasmin were found to vary significantly between groups at $q < 0.05$. Cop-
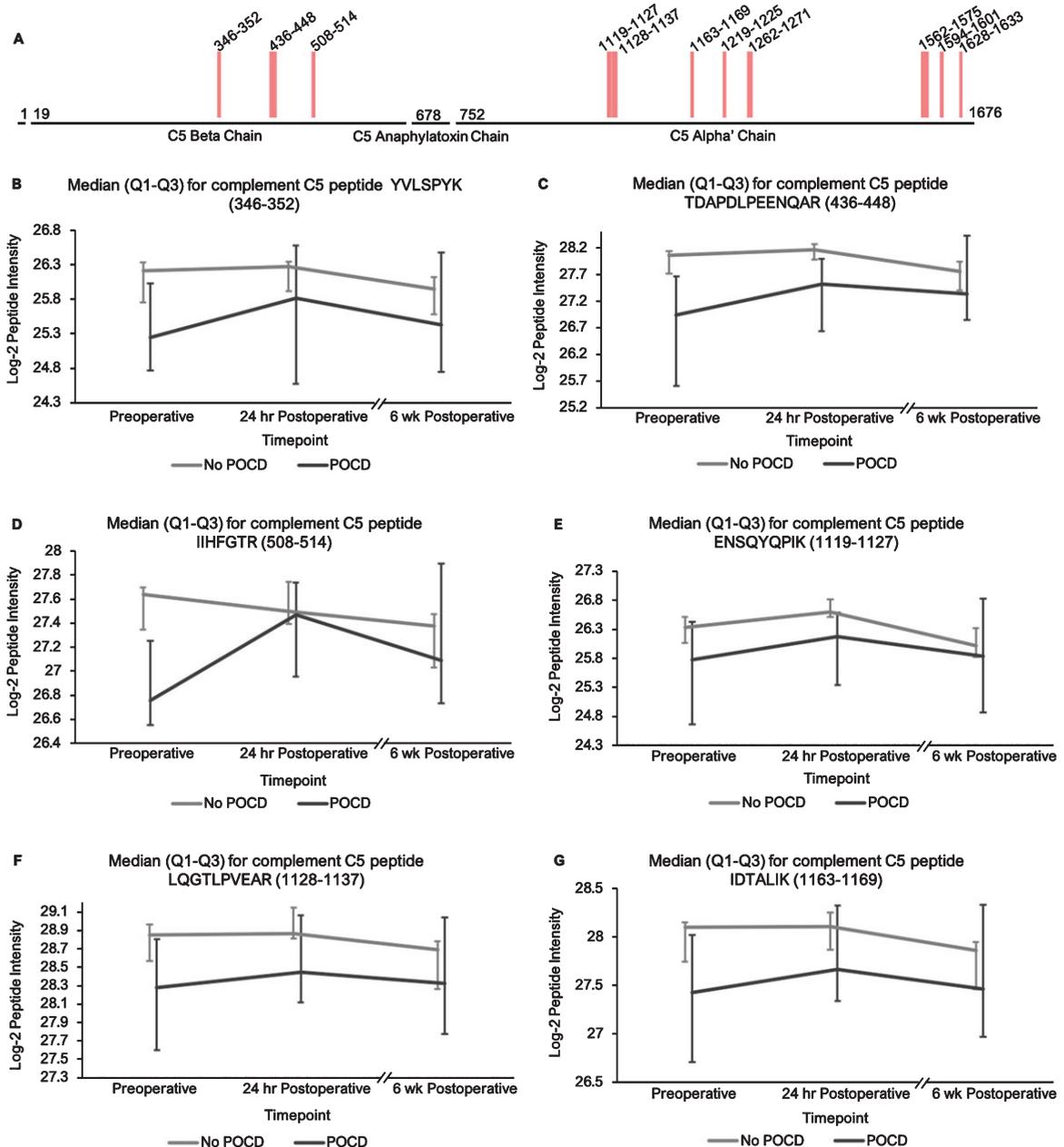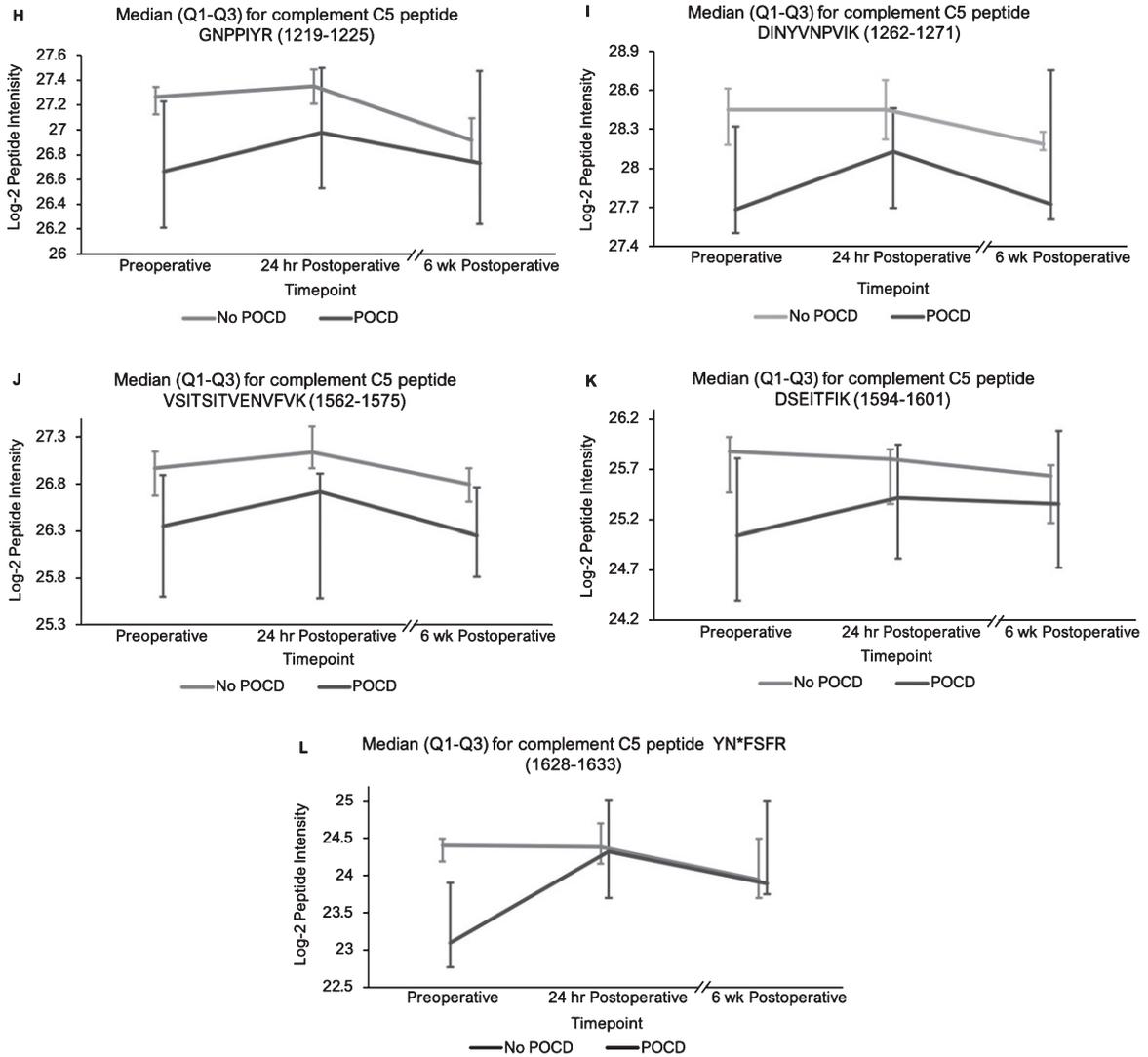

Fig. 1. (*Continued*)

Fig. 1. Complement C5 peptide locations and intensity trends. A) A map of complement C5 showing the locations of its 11 peptides with (q < 0.25) in the linear mixed models. Peptides 1–3 are located on the beta subunit, and 4–11 are located on the alpha subunit. B-L) Graphs comparing median C5 peptide intensities between POCD and non-POCD groups across all three time points. Vertical bars represent interquartile range.

per storage and regulation abnormalities have been implicated in the pathogenesis of AD (reviewed) [57] and HIV-associated neurocognitive disorder [58], and alterations in ceruloplasmin activity have been associated with increased AD risk [59, 60]. Finally, the axonal secretory sorting receptor secretogranin-III, represented by a single peptide with q < 0.05, has been implicated in the mechanisms driving amyloid-mediated neurodegeneration in AD [61]. To our knowledge, these proteins have not previously been previously associated with POCD. Targeted proteomic studies to determine their roles in periop-erative neurocognitive disorders are thus warranted.

Our ability to identify additional proteins and path-ways associated with POCD in this pilot study was limited by a high degree of variance in peptide intensi-ties among the participants, and there was no peptide that showed intensity differences between groups at any single time point. Despite this limitation, analysis of our results revealed two noteworthy trends. First, among all complement proteins containing peptides with significantly different intensities in our mixed models, the mean baseline peptide levels were lower in patients who later developed POCD. Second, over the course of six weeks, there was a clear trend toward convergence of these peptide intensities for all of the
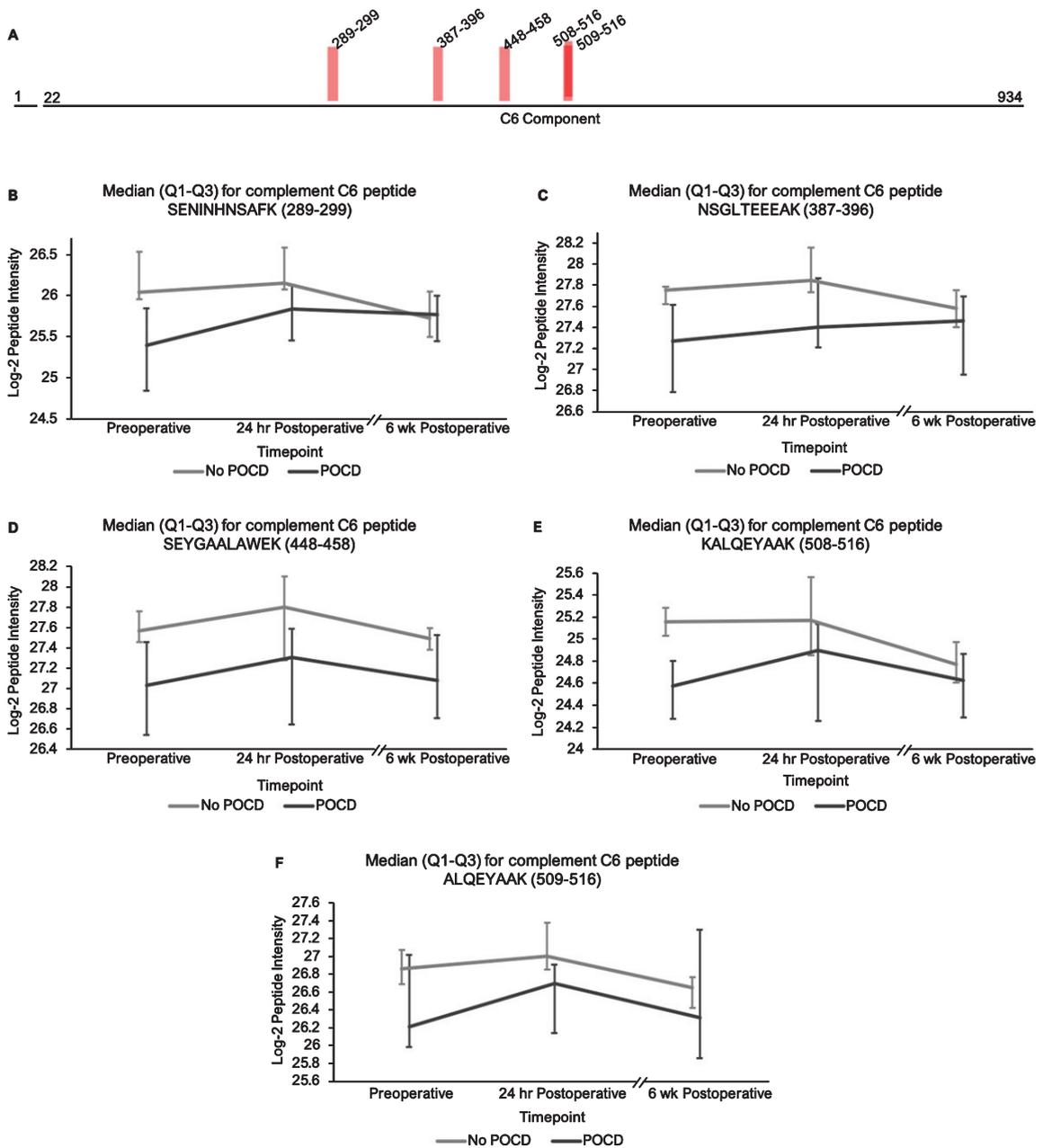
Fig. 2. Complement C6 peptide locations and intensity trends. A) A map of complement C6 showing the locations of its five peptides with q < 0.25 in the linear mixed models. B-F) Graphs comparing median C6 peptide intensities between POCD and non-POCD groups across all three time points. Vertical bars represent interquartile range.

proteins except complement factor H, which further diverged by the six-week time point. The consistency of these trends supports their validity despite considerable peptide variance and the relatively small study size. These data may prove useful for planning future studies using unbiased proteomic analyses on perioperative CSF samples. For example, a power analysis on complement C5 and C6 peptide intensi-

ties, with $\alpha = 0.0001$ to account for multiple testing, indicates that group sizes of > 31 patients would have 80% power to reveal significant differences between baseline peptide intensities (calculated for C6 peptide KALQEYAAK, with a difference of $1.419*10^7$ between means).

The hypothesis that complement plays a role in perioperative neurocognitive disorders aligns with
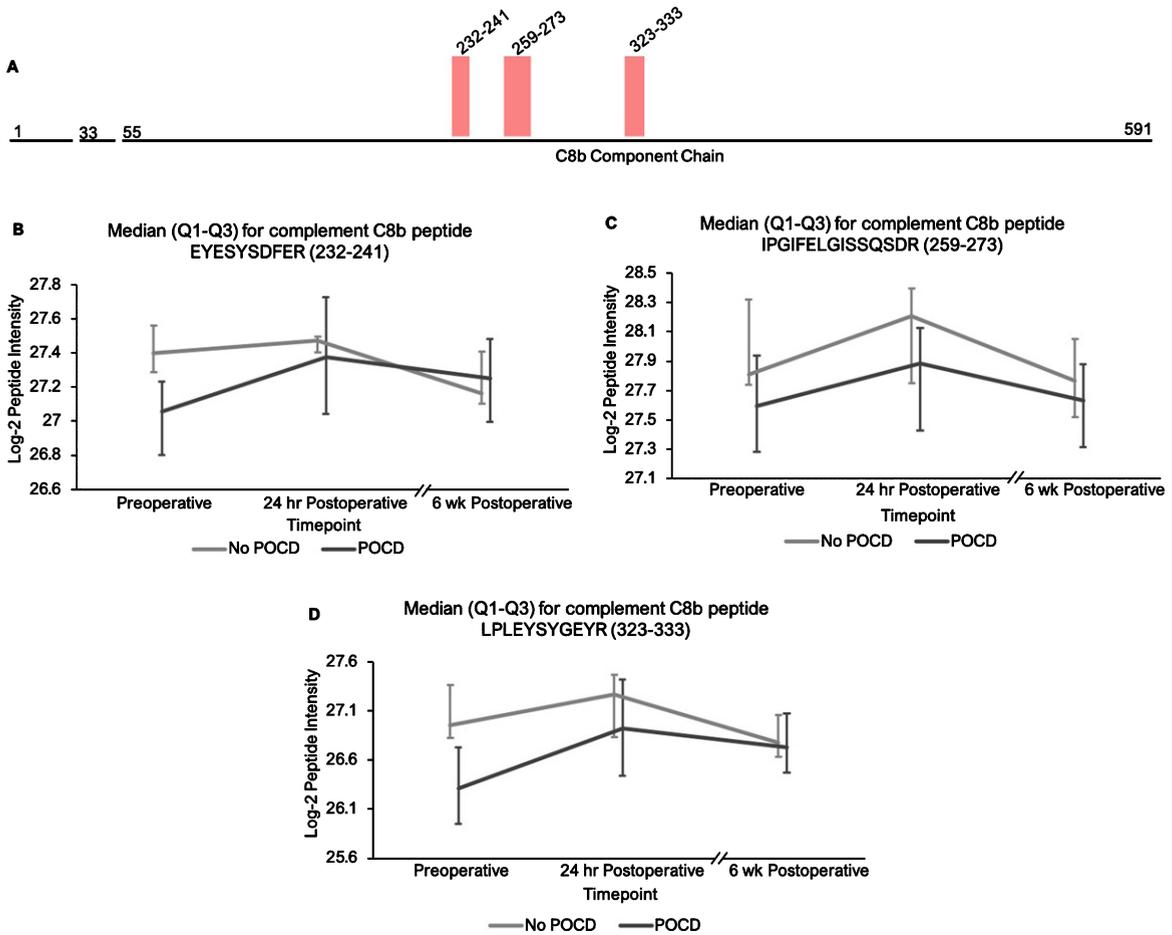
Fig. 3. Complement C8b peptide locations and intensity trends. A) A map of complement C8b showing the locations of its three peptides with $q < 0.25$ in the linear mixed model. B-D) Graphs comparing median C8b peptide intensities between POCD and non-POCD groups across all three time points. Vertical bars represent interquartile range.

current animal models of surgery-induced neuroinflammation and cognitive decline [62]. Indeed, surgery activates the systemic complement pathway in animal models and cardiac surgery patients. Complement regulates brain development and homeostasis by driving microglial synaptic phagocytosis [63], and in murine models, complement-dependent synaptic pruning is critical for optimizing cognitive performance by reducing excessive synapse numbers that can cause epilepsy [64, 65]. However, abnormal CNS complement activity has also been revealed in several neurocognitive disease states as a neuroinflammatory trigger for microglial activation and neuronal damage [66–68]. A role for complement in perioperative neurocognitive disorders would fit with the theory that these disorders are driven by neuroinflammation [1, 69]. Indeed, murine model studies have shown that levels of complement C3, an initiator of the complement cascade, and levels of the receptor for its cleavage product (C3aR) are elevated after orthopedic surgery, and these increases have been shown to contribute to cognitive dysfunction in mouse POCD models [62]. Similarly, elevated baseline CSF C3 levels have been associated with higher rates of postoperative delirium in hip fracture patients [70], and critically-ill patients with delirium have been found to exhibit upregulated CSF complement levels [71]. Our results generally fit with these prior studies, though we identified the largest difference in complement protein-derived peptides between patients with versus without POCD before rather than after surgery. In contrast, the mouse studies described above largely showed complement protein and pathway differences after surgery that correlated with cognitive outcomes. These temporal differences could reflect species differences between mice and humans, or the fact that most laboratory mouse strains are genetically inbred, while most

human populations are considerably more genetically diverse. Nonetheless, it is premature to conclude that there is a significant mouse versus human difference in the temporal role of CNS complement in perioperative neurocognitive disorders based on the data from only 14 patients studied here. Larger future human studies will be necessary to more carefully delineate the temporal role of complement in human perioperative neurocognitive disorders.

In addition to the complement peptides that differed between groups, several non-complement factors with known pro-inflammatory and/or hemostatic functions were identified by our linear mixed models as trending toward significance (q < 0.25) between the patients with versus without POCD over the six-week period. Notably, fibrinogen and its cleavage products are known to contribute to inflammation in the CNS by a variety of mechanisms including microglial activation [72, 73], neuronal damage [74], interactions with amyloid-β [75], and disrup-

tion of the blood-brain barrier [76]. In fact, alterations in CNS fibrinogen biology have been implicated in the pathogenesis of neurological, neurocognitive, and psychiatric disorders including multiple sclerosis [77], traumatic brain injury [78], AD [73, 79], and depression [80]. Likewise, coagulation factor V, a central mediator of hemostasis, has been previously linked to delirium pathogenesis [81]. Further, plasminogen has been shown to potentiate neuroinflammation [82, 83] and AD-related pathology [82], and elevated serum kininogen has been associated with depression [80]. As with complement, our data provide hypothesis-generating evidence for a potential relationship between POCD and dysregulation of these inflammatory and hemostatic factors.

Several limitations apply to this study. First, although the CSF analyses presented here suggest differential changes in peptides levels from complement and coagulation-related proteins between patients with versus without POCD, it is possible that these
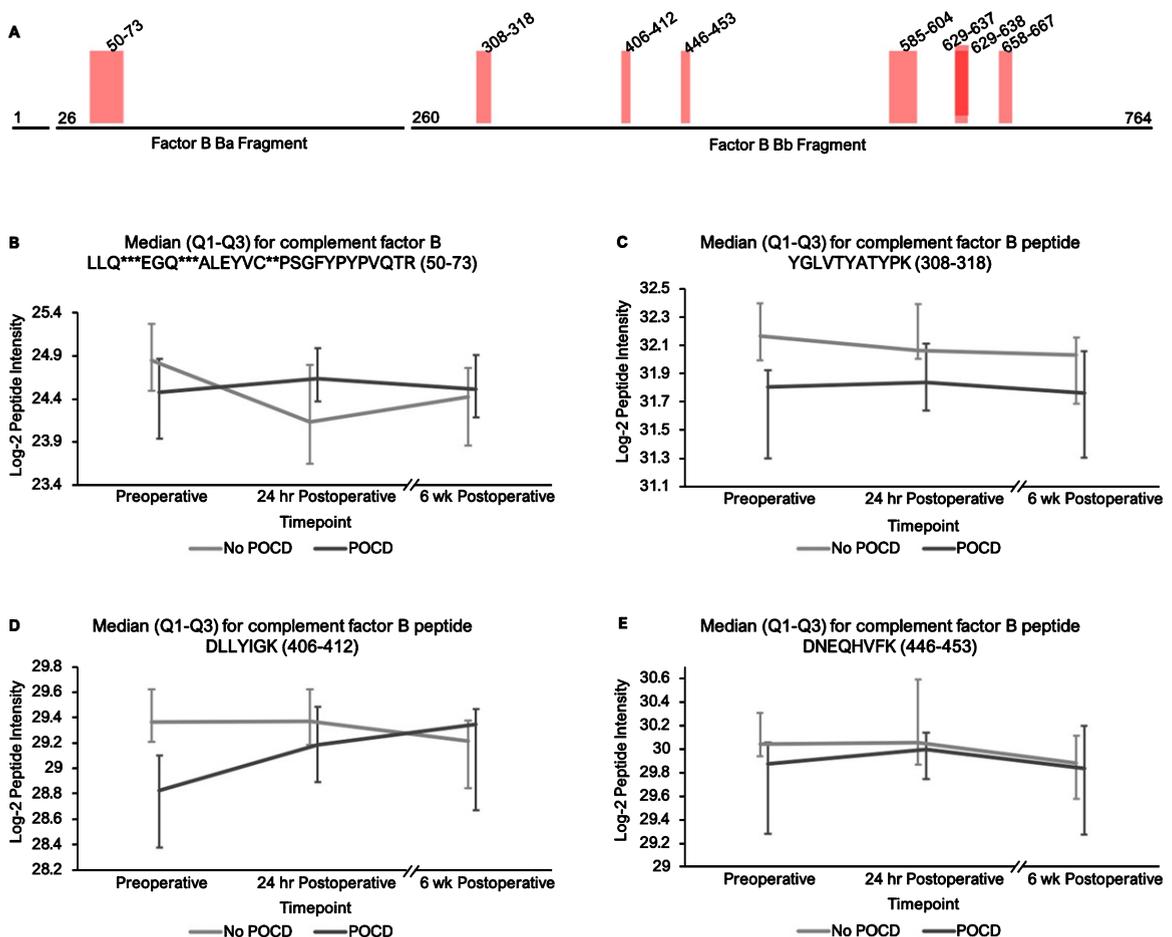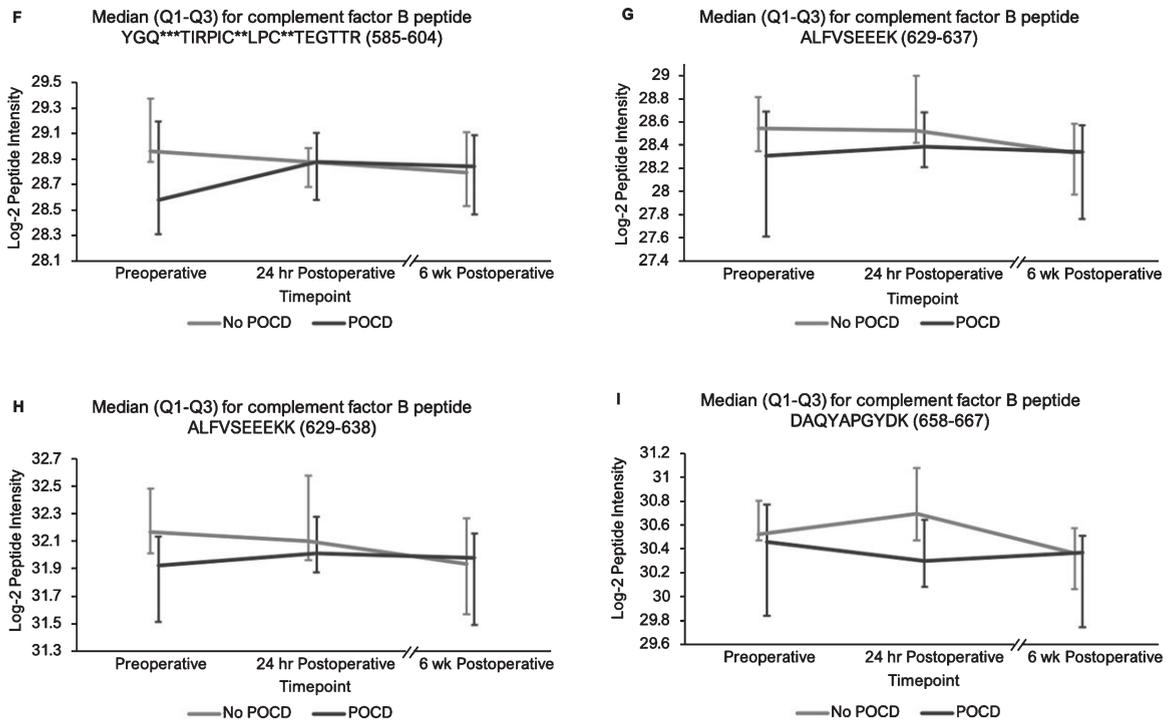

Fig. 4. (*Continued*)

Fig. 4. Complement factor B peptide locations and intensity trends. A) A map of complement factor B showing the locations of its eight peptides with q < 0.25 in the linear mixed model. Seven of the eight peptides represent portions of its Bb fragment. B-I) Graphs comparing median factor b peptide intensities between POCD and non-POCD groups across all three time points. Vertical bars represent interquartile range. Post-translational modifications: *Deamidation, **Carbamidomethylation, ***Oxidation.

changes could reflect non-causal associations. In essence, these pathways may be markers of POCD rather than causative factors. Second, like other mass spectrometry-based analyses, the intensities measured in this study reflect relative peptide levels rather than quantitative concentration measurements. Thus, while our unbiased approach has identified candidate proteins with suspected involvement in POCD, precise protein levels and inter-protein comparisons will require additional targeted studies (i.e., proteomic studies with internal controls designed for precise quantification) or quantitation of specific analytes with ELISA-based assays. Furthermore, aside from several quality validation tests and two samples run in duplicate, all other mass spectrometry sample measurements in this study were run in singlicate, increasing the possibility that technical variation may affect our measurements. Third, non-protein small-molecule inflammatory mediators such as prostanoids, leukotrienes, and reactive oxygen species, which could contribute to POCD, cannot be assessed with the proteomic approach used here. Indeed, we recently found significant 24 h postoperative changes in CSF levels of arachidonic acid pathway members using a "lipidomics" approach [84], so future stud-

ies should examine the interplay between CSF lipid and protein mediators in perioperative neurocognitive disorders. Likewise, the immunodepletion protocol used here to remove high-abundancy plasma proteins, which can interfere with the detection of low abundance proteins, may also have prevented identification of any highly abundant proteins involved in POCD pathogenesis. Future studies attempting to examine the role of high abundance proteins in perioperative neurocognitive disorders may thus benefit from avoiding immunodepletion. Fourth, the results of this exploratory study are preliminary, and larger, properly powered future studies are needed to thoroughly assess the role of these proteins and pathways in POCD and/or other perioperative neurocognitive disorders. Such studies will be expensive; the proteomic assays and immunodepletions used in this report cost just under $700 per sample (or slightly below $29,000 for all 42 CSF samples) in addition to the costs of enrolling these patients in the MA DCO-PC study, collecting CSF, and data analysis. Nonetheless, there are savings related to economy of scale, and the present cost of performing these assays may drop to $500 or less per sample if hundreds of samples are run in bulk. Thus, performing unbiased

proteomics on CSF samples across three different time points from two groups of 32 patients each (i.e., one group with and one group without POCD) may incur approximately $100,000 in assay costs alone. Fifth, it is unclear whether the differential changes in CSF protein levels observed in this study are driven primarily by changes in expression, activity, or turnover initiated within the CNS, versus peripheral inflammation and activation of the coagulation and complement cascades after surgery that crosses the blood-brain barrier into the CNS. Further research comparing postoperative changes in both the CSF and plasma proteomes at multiple simultaneous time points may help evaluate these two different possibilities.

In conclusion, this pilot study suggests that unbiased CSF proteomic analyses can be used to study potential mechanisms underlying perioperative neurocognitive disorders and provides preliminary hypothesis-generating evidence to support future investigation of CNS complement and coagulation pathway activation in these conditions. Additionally, the data reported here may guide sample size calculations for future studies to definitively investigate the role of CSF complement and coagulation pathway changes in POCD and other perioperative neurocognitive disorders.

ACKNOWLEDGMENTS

SUPPLEMENTARY MATERIAL

The supplementary material is available in the electronic version of this article: https://dx.doi.org/10.3233/JAD-201544.

REFERENCES

[1] Berger M, Nadler JW, Browndyke J, Terrando N, Ponnusamy V, Cohen HJ, Whitson HE, Mathew JP (2015) Postoperative cognitive dysfunction: Minding the gaps in our knowledge of a common postoperative complication in the elderly. *Anesthesiol Clin* **33**, 517-550.

[2] Evered L, Silbert B, Knopman DS, Scott DA, DeKosky ST, Rasmussen LS, Oh ES, Crosby G, Berger M, Eckenhoff RG (2018) Recommendations for the nomenclature of cognitive change associated with anaesthesia and surgery-2018. *Can J Anaesth* **65**, 1248-1257.

[3] Berger M, Burke J, Eckenhoff R, Mathew J (2014) Alzheimer's disease, anesthesia, and surgery: A clinically focused review. *J Cardiothorac Vasc Anesth* **28**, 1609-1623.

[4] Phillips-Bute B, Mathew JP, Blumenthal JA, Grocott HP, Laskowitz DT, Jones RH, Mark DB, Newman MF (2006) Association of neurocognitive function and quality of life 1 year after coronary artery bypass graft (CABG) surgery. *Psychosom Med* **68**, 369-375.

[5] Newman MF, Grocott HP, Mathew JP, White WD, Landolfo K, Reves JG, Laskowitz DT, Mark DB, Blumenthal JA (2001) Report of the substudy assessing the impact of neurocognitive function on quality of life 5 years after cardiac surgery. *Stroke* **32**, 2874-2881.

[6] Newman MF, Kirchner JL, Phillips-Bute B, Gaver V, Grocott H, Jones RH, Mark DB, Reves JG, Blumenthal JA (2001) Longitudinal assessment of neurocognitive function after coronary-artery bypass surgery. *N Engl J Med* **344**, 395-402.

[7] Monk TG, Weldon BC, Garvan CW, Dede DE, van der Aa MT, Heilman KM, Gravenstein JS (2008) Predictors of cognitive dysfunction after major noncardiac surgery. *Anesthesiology* **108**, 18-30.

[8] Cullen KA, Hall MJ, Golosinskiy A (2009) Ambulatory surgery in the United States, 2006. *Natl Health Stat Report*, pp. 1-25.

[9] Calsolaro V, Edison P (2016) Neuroinflammation in Alzheimer's disease: Current evidence and future directions. *Alzheimers Dement* **12**, 719-732.

[10] Ramaglia V, Hughes TR, Donev RM, Ruseva MM, Wu X, Huitinga I, Baas F, Neal JW, Morgan BP (2012) C3-dependent mechanism of microglial priming relevant to multiple sclerosis. *Proc Natl Acad Sci U S A* **109**, 965.

[11] Fominykh V, Brylev L, Gaskin V, Luzin R, Yakovlev A, Komoltsev I, Belousova I, Rosliakova A, Guekht A, Gulyaeva N (2019) Neuronal damage and neuroinflammation markers in patients with autoimmune encephalitis and multiple sclerosis. *Metab Brain Dis* **34**, 1473-1485.

[12] Terrando N, Monaco C, Ma D, Foxwell BM, Feldmann M, Maze M (2010) Tumor necrosis factor-alpha triggers a cytokine cascade yielding postoperative cognitive decline. *Proc Natl Acad Sci U S A* **107**, 20518-20522.

[13] Hirsch J, Vacas S, Terrando N, Yuan M, Sands LP, Kramer J, Bozic K, Maze MM, Leung JM (2016) Perioperative cerebrospinal fluid and plasma inflammatory markers after orthopedic surgery. *J Neuroinflammation* **13**, 211.

[14] Tang JX, Baranov D, Hammond M, Shaw LM, Eckenhoff MF, Eckenhoff RG (2011) Human Alzheimer and inflammation biomarkers after anesthesia and surgery. *Anesthesiology* **115**, 727-732.

[15] Terrando N, Eriksson LI, Ryu JK, Yang T, Monaco C, Feldmann M, Jonsson Fagerlund M, Charo IF, Akassoglou K, Maze M (2011) Resolving postoperative neuroinflammation and cognitive decline. *Ann Neurol* **70**, 986-995.

[16] Mietani K, Sumitani M, Ogata T, Shimojo N, Inoue R, Abe H, Kawamura G, Yamada Y (2019) Dysfunction of the blood-brain barrier in postoperative delirium patients, referring to the axonal damage biomarker phosphorylated neurofilament heavy subunit. *PLoS One* **14**, e0222721.

[17] Tang JX, Mardini F, Janik LS, Garrity ST, Li RQ, Bachlani G, Eckenhoff RG, Eckenhoff MF (2013) Modulation of murine Alzheimer pathogenesis and behavior by surgery. *Ann Surg* **257**, 439-448.

[18] Berger M, Nadler JW, Friedman A, McDonagh DL, Bennett ER, Cooter M, Qi W, Laskowitz DT, Ponnusamy V, Newman MF, Shaw LM, Warner DS, Mathew JP, James ML (2016) The effect of propofol versus isoflurane anesthesia on human cerebrospinal fluid markers of Alzheimer's disease: Results of a randomized trial. *J Alzheimers Dis* **52**, 1299-1310.

[19] Berger M, Ponnusamy V, Greene N, Cooter M, Nadler JW, Friedman A, McDonagh DL, Laskowitz DT, Newman MF, Shaw LM, Warner DS, Mathew JP, James ML, MAD-PIA Investigators (2017) The effect of propofol vs. isoflurane anesthesia on postoperative changes in cerebrospinal fluid cytokine levels: Results from a randomized trial. *Front Immunol* **8**, 1528.

[20] Xie Z, McAuliffe S, Swain CA, Ward SAP, Crosby CA, Zheng H, Sherman J, Dong Y, Zhang Y, Sunder N, Burke D, Washicosky KJ, Tanzi RE, Marcantonio ER (2013) Cerebrospinal fluid aβ to tau ratio and postoperative cognitive change. *Ann Surg* **258**, 364-369.

[21] Cunningham EL, McGuinness B, McAuley DF, Toombs J, Mawhinney T, O'Brien S, Beverland D, Schott JM, Lunn MP, Zetterberg H, Passmore AP (2019) CSF Beta-amyloid 1-42 concentration predicts delirium following elective arthroplasty surgery in an observational cohort study. *Ann Surg* **269**, 1200-1205.

[22] Evered L, Silbert B, Scott DA, Ames D, Maruff P, Blennow K (2016) Cerebrospinal fluid biomarker for Alzheimer disease predicts postoperative cognitive dysfunction. *Anesthesiology* **124**, 353-361.

[23] Rush J, Moritz A, Lee KA, Guo A, Goss VL, Spek EJ, Zhang H, Zha XM, Polakiewicz RD, Comb MJ (2005) Immunoaffinity profiling of tyrosine phosphorylation in cancer cells. *Nat Biotechnol* **23**, 94-101.

[24] Wang M, Beckmann ND, Roussos P, Wang E, Zhou X, Wang Q, Ming C, Neff R, Ma W, Fullard JF, Hauberg ME, Bendl J, Peters MA, Logsdon B, Wang P, Mahajan M, Mangravite LM, Dammer EB, Duong DM, Lah JJ, Seyfried NT, Levey AI, Buxbaum JD, Ehrlich M, Gandy S, Katsel P, Haroutunian V, Schadt E, Zhang B (2018) The Mount Sinai cohort of large-scale genomic, transcriptomic and proteomic data in Alzheimer's disease. *Sci Data* **5**, 180185.

[25] Johnson ECB, Dammer EB, Duong DM, Yin L, Thambisetty M, Troncoso JC, Lah JJ, Levey AI, Seyfried NT (2018) Deep proteomic network analysis of Alzheimer's disease brain reveals alterations in RNA binding proteins and RNA splicing associated with disease. *Mol Neurodegener* **13**, 52.

[26] Ringman JM, Schulman H, Becker C, Jones T, Bai Y, Immermann F, Cole G, Sokolow S, Gylys K, Geschwind DH, Cummings JL, Wan HI (2012) Proteomic changes in cerebrospinal fluid of presymptomatic and affected persons carrying familial Alzheimer disease mutations. *Arch Neurol* **69**, 96-104.

[27] van der Ende EL, Meeter LH, Stingl C, van Rooij JGJ, Stoop MP, Nijholt DAT, Sanchez-Valle R, Graff C, Oijerstedt L, Grossman M, McMillan C, Pijnenburg YAL, Laforce R,

Jr., Binetti G, Benussi L, Ghidoni R, Luider TM, Seelaar H, van Swieten JC (2019) Novel CSF biomarkers in genetic frontotemporal dementia identified by proteomics. *Ann Clin Transl Neurol* **6**, 698-707.

[28] Umoh ME, Dammer EB, Dai J, Duong DM, Lah JJ, Levey AI, Gearing M, Glass JD, Seyfried NT (2018) A proteomic network approach across the ALS-FTD disease spectrum resolves clinical phenotypes and genetic vulnerability in human brain. *EMBO Mol Med* **10**, 48-62.

[29] Henderson MX, Chung CH, Riddle DM, Zhang B, Gathagan RJ, Seeholzer SH, Trojanowski JQ, Lee VMY (2017) Unbiased proteomics of early Lewy body formation model implicates active microtubule affinity-regulating kinases (MARKs) in synucleinopathies. *J Neurosci* **37**, 5870-5884.

[30] Guha D, Lorenz DR, Misra V, Chettimada S, Morgello S, Gabuzda D (2019) Proteomic analysis of cerebrospinal fluid extracellular vesicles reveals synaptic injury, inflammation, and stress response markers in HIV patients with cognitive impairment. *J Neuroinflammation* **16**, 254-254.

[31] Fernandez-Irigoyen J, Zelaya MV, Santamaria E (2014) Applying mass spectrometry-based qualitative proteomics to human amygdaloid complex. *Front Cell Neurosci* **8**, 80.

[32] Muraoka S, Jedrychowski MP, Tatebe H, DeLeo AM, Ikezu S, Tokuda T, Gygi SP, Stern RA, Ikezu T (2019) Proteomic profiling of extracellular vesicles isolated from cerebrospinal fluid of former National Football League players at risk for chronic traumatic encephalopathy. *Front Neurosci* **13**, 1059.

[33] Giattino CM, Gardner JE, Sbahi FM, Roberts KC, Cooter M, Moretti E, Browndyke JN, Mathew JP, Woldorff MG, Berger M (2017) Intraoperative frontal alpha-band power correlates with preoperative neurocognitive function in older adults. *Front Syst Neurosci* **11**, 24.

[34] Mathew JP, White WD, Schinderle DB, Podgoreanu MV, Berger M, Milano CA, Laskowitz DT, Stafford-Smith M, Blumenthal JA, Newman MF (2013) Intraoperative magnesium administration does not improve neurocognitive function after cardiac surgery. *Stroke* **44**, 3407-3413.

[35] Berger M, Oyeyemi D, Olurinde MO, Whitson HE, Weinhold KJ, Woldorff MG, Lipsitz LA, Moretti E, Giattino CM, Roberts KC, Zhou J, Bunning T, Ferrandino M, Scheri RP, Cooter M, Chan C, Cabeza R, Browndyke JN, Murdoch DM, Devinney MJ, Shaw LM, Cohen HJ, Mathew JP, INTUIT Investigators (2019) The INTUIT Study: Investigating neuroinflammation underlying postoperative cognitive dysfunction. *J Am Geriatr Soc* **67**, 794-798.

[36] McDonagh DL, Mathew JP, White WD, Phillips-Bute B, Laskowitz DT, Podgoreanu MV, Newman MF, Neurologic Outcome Research Group (2010) Cognitive function after major noncardiac surgery, apolipoprotein E4 genotype, and biomarkers of brain injury. *Anesthesiology* **112**, 852-859.

[37] Klinger RY, Cooter M, Berger M, Podgoreanu MV, Stafford-Smith M, Ortel TL, Welsby IJ, Levy JH, Rinder HM, Newman MF, Mathew JP, Neurologic Outcomes Research Group (NORG) of The Duke Heart Center (2016) Effect of intravenous lidocaine on the transcerebral inflammatory response during cardiac surgery: A randomized-controlled trial. *Can J Anaesth* **63**, 1223-1232.

[38] Browndyke JN, Berger M, Smith PJ, Harshbarger TB, Monge ZA, Panchal V, Bisanar TL, Glower DD, Alexander JH, Cabeza R, Welsh-Bohmer K, Newman MF, Mathew JP, Duke Neurologic Outcomes Research Group (2018) Task-related changes in degree centrality and local coherence of

the posterior cingulate cortex after major cardiac surgery in older adults. *Hum Brain Mapp* **39**, 985-1003.

[39] Klinger RY, James OG, Borges-Neto S, Bisanar T, Li Y-J, Qi W, Berger M, Terrando N, Newman MF, Doraiswamy PM, Mathew JP, Alzheimer's Disease Neuroimaging Initiative (ADNI) Study Group; Neurologic Outcomes Research Group (NORG) (2018) 18F-florbetapir positron emission tomography-determined cerebral β-amyloid deposition and neurocognitive performance after cardiac surgery. *Anesthesiology* **128**, 728-744.

[40] Berger M, Murdoch DM, Staats JS, Chan C, Thomas JP, Garrigues GE, Browndyke JN, Cooter M, Quinones QJ, Mathew JP, Weinhold KJ (2019) Flow cytometry characterization of cerebrospinal fluid monocytes in patients with postoperative cognitive dysfunction: A pilot study. *Anesth Analg* **129**, e150-e154.

[41] Smith PJ, Browndyke JN, Monge ZA, Harshbarger TB, James ML, Gaca JG, Alexander JH, Berger MM, Newman MF, Milano CA, Mathew JP, Neurologic Outcomes Research Group (2019) Longitudinal changes in regional cerebral perfusion and cognition after cardiac operation. *Ann Thorac Surg* **107**, 112-118.

[42] Browndyke JN, Berger M, Harshbarger TB, Smith PJ, White W, Bisanar TL, Alexander JH, Gaca JG, Welsh-Bohmer K, Newman MF, Mathew JP (2017) Resting-state functional connectivity and cognition after major cardiac surgery in older adults without preoperative cognitive impairment: Preliminary findings. *J Am Geriatr Soc* **65**, e6-e12.

[43] Avidan MS, Xiong C, Evers AS (2010) Postoperative cognitive decline: The unsubstantiated phenotype. *Anesthesiology* **113**, 1246-1248; author reply 1248-1250.

[44] Yang T, Xu G, Newton PT, Chagin AS, Mkrtchian S, Carlstrom M, Zhang XM, Harris RA, Cooter M, Berger M, Maddipati KR, Akassoglou K, Terrando N (2019) Maresin 1 attenuates neuroinflammation in a mouse model of perioperative neurocognitive disorders. *Br J Anaesth* **122**, 350-360.

[45] Nobuhara CK, Bullock WM, Bunning T, Colin B, Cooter M, Devinney MJ, Ferrandino MN, Gadsden J, Garrigues G, Habib AS, Moretti E, Moul J, Ohlendorf B, Sandler A, Scheri R, Sharma B, Thomas JP, Young C, Mathew JP, Berger M (2020) A protocol to reduce self-reported pain scores and adverse events following lumbar punctures in older adults. *J Neurol* **267**, 2002-2006.

[46] Storey JD (2003) The positive false discovery rate: A Bayesian interpretation and the q -value. *Ann Statist* **31**, 2013-2035.

[47] Benjamini Y, Hochberg Y (1995) Controlling the false discovery rate: A practical and powerful approach to multiple testing. *J R Stat Soc Series B Methodol* **57**, 289-300.

[48] Storey JD (2002) A direct approach to false discovery rates. *J R Stat Soc Series B Stat Methodol* **64**, 479-498.

[49] Huang da W, Sherman BT, Lempicki RA (2009) Systematic and integrative analysis of large gene lists using DAVID bioinformatics resources. *Nat Protoc* **4**, 44-57.

[50] Huang da W, Sherman BT, Lempicki RA (2009) Bioinformatics enrichment tools: Paths toward the comprehensive functional analysis of large gene lists. *Nucleic Acids Res* **37**, 1-13.

[51] Mi W, Pawlik M, Sastre M, Jung SS, Radvinsky DS, Klein AM, Sommer J, Schmidt SD, Nixon RA, Mathews PM, Levy E (2007) Cystatin C inhibits amyloid-β deposition in Alzheimer's disease mouse models. *Nat Genet* **39**, 1440-1442.

[52] Sundelöf J, Arnlöv J, Ingelsson E, Sundström J, Basu S, Zethelius B, Larsson A, Irizarry MC, Giedraitis V,

Rönnemaa E, Degerman-Gunnarsson M, Hyman BT, Basun H, Kilander L, Lannfelt L (2008) Serum cystatin C and the risk of Alzheimer disease in elderly men. *Neurology* **71**, 1072-1079.

[53] Kaur G, Levy E (2012) Cystatin C in Alzheimer's disease. *Front Mol Neurosci* **5**, 79-79.

[54] Hu WD, Chen J, Mao CJ, Feng P, Yang YP, Luo WF, Liu CF (2016) Elevated cystatin C levels are associated with cognitive impairment and progression of Parkinson disease. *Cogn Behav Neurol* **29**, 144-149.

[55] Guo D-X, Zhu Z-B, Zhong C-K, Bu X-Q, Chen L-H, Xu T, Guo L-B, Zhang J-T, Li D, Zhang J-H, Ju Z, Chen C-S, Chen J, Zhang Y-H, He J (2020) Serum cystatin C levels are negatively correlated with post-stroke cognitive dysfunction. *Neural Regen Res* **15**, 922-928.

[56] Kalayjian RC, Robertson KR, Albert JM, Fichtenbaum CJ, Brown TT, Taiwo BO (2019) Plasma cystatin C associates with HIV-associated neurocognitive disorder but is a poor diagnostic marker in antiretroviral therapy-treated individuals. *J Acquir Immune Defic Syndr* **81**, e49-e54.

[57] Sensi SL, Granzotto A, Siotto M, Squitti R (2018) Copper and zinc dysregulation in Alzheimer's disease. *Trends Pharmacol Sci* **39**, 1049-1063.

[58] Kallianpur AR, Gittleman H, Letendre S, Ellis R, Barnholtz-Sloan JS, Bush WS, Heaton R, Samuels DC, Franklin DR, Jr., Rosario-Cookson D, Clifford DB, Collier AC, Gelman B, Marra CM, McArthur JC, McCutchan JA, Morgello S, Grant I, Simpson D, Connor JR, Hulgan T (2019) Cerebrospinal fluid ceruloplasmin, haptoglobin, and vascular endothelial growth factor are associated with neurocognitive impairment in adults with HIV infection. *Mol Neurobiol* **56**, 3808-3818.

[59] Siotto M, Simonelli I, Pasqualetti P, Mariani S, Caprara D, Bucossi S, Ventriglia M, Molinario R, Antenucci M, Rongioletti M, Rossini PM, Squitti R (2016) Association between serum ceruloplasmin specific activity and risk of Alzheimer's disease. *J Alzheimers Dis* **50**, 1181-1189.

[60] Diouf I, Bush AI, Ayton S (2020) Cerebrospinal fluid ceruloplasmin levels predict cognitive decline and brain atrophy in people with underlying β-amyloid pathology. *Neurobiol Dis* **139**, 104810.

[61] Plá V, Paco S, Ghezali G, Ciria V, Pozas E, Ferrer I, Aguado F (2013) Secretory sorting receptors carboxypeptidase E and secretogranin III in amyloid β-associated neural degeneration in Alzheimer's disease. *Brain Pathol* **23**, 274-284.

[62] Xiong C, Liu J, Lin D, Zhang J, Terrando N, Wu A (2018) Complement activation contributes to perioperative neurocognitive disorders in mice. *J Neuroinflammation* **15**, 254.

[63] Schafer DP, Lehrman EK, Kautzman AG, Koyama R, Mardinly AR, Yamasaki R, Ransohoff RM, Greenberg ME, Barres BA, Stevens B (2012) Microglia sculpt postnatal neural circuits in an activity and complement-dependent manner. *Neuron* **74**, 691-705.

[64] Shi Q, Colodner KJ, Matousek SB, Merry K, Hong S, Kenison JE, Frost JL, Le KX, Li S, Dodart JC, Caldarone BJ, Stevens B, Lemere CA (2015) Complement C3-deficient mice fail to display age-related hippocampal decline. *J Neurosci* **35**, 13029-13042.

[65] Chu Y, Jin X, Parada I, Pesic A, Stevens B, Barres B, Prince DA (2010) Enhanced synaptic connectivity and epilepsy in C1q knockout mice. *Proc Natl Acad Sci U S A* **107**, 7975-7980.

[66] Alawieh A, Langley EF, Tomlinson S (2018) Targeted complement inhibition salvages stressed neurons and inhibits

neuroinflammation after stroke in mice. *Sci Transl Med* **10**, eaao6459.

[67] Hong S, Beja-Glasser VF, Nfonoyim BM, Frouin A, Li S, Ramakrishnan S, Merry KM, Shi Q, Rosenthal A, Barres BA, Lemere CA, Selkoe DJ, Stevens B (2016) Complement and microglia mediate early synapse loss in Alzheimer mouse models. *Science* **352**, 712.

[68] Sekar A, Bialas AR, de Rivera H, Davis A, Hammond TR, Kamitaki N, Tooley K, Presumey J, Baum M, Van Doren V, Genovese G, Rose SA, Handsaker RE, Daly MJ, Carroll MC, Stevens B, McCarroll SA (2016) Schizophrenia risk from complex variation of complement component 4. *Nature* **530**, 177-183.

[69] Subramaniyan S, Terrando N (2019) Neuroinflammation and perioperative neurocognitive disorders. *Anesth Analg* **128**, 781-788.

[70] Westhoff D, Witlox J, van Aalst C, Scholtens RM, de Rooij SE, van Munster BC, de Jonghe JFM, Houdijk APJ, Eikelenboom P, van Westerloo DJ, van de Beek D, van Gool WA, Koenderman L (2015) Preoperative protein profiles in cerebrospinal fluid in elderly hip fracture patients at risk for delirium: A proteomics and validation study. *BBA Clin* **4**, 115-122.

[71] Poljak A, Hill M, Hall RJ, MacLullich AM, Raftery MJ, Tai J, Yan S, Caplan GA (2014) Quantitative proteomics of delirium cerebrospinal fluid. *Transl Psychiatry* **4**, e477.

[72] Piers TM, East E, Villegas-Llerena C, Sevastou IG, Matarin M, Hardy J, Pocock JM (2018) Soluble fibrinogen triggers non-cell autonomous ER stress-mediated microglial-induced neurotoxicity. *Front Cell Neurosci* **12**, 404.

[73] Merlini M, Rafalski VA, Rios Coronado PE, Gill TM, Ellisman M, Muthukumar G, Subramanian KS, Ryu JK, Syme CA, Davalos D, Seeley WW, Mucke L, Nelson RB, Akassoglou K (2019) Fibrinogen induces microglia-mediated spine elimination and cognitive impairment in an Alzheimer's disease model. *Neuron* **101**, 1099-1108.e1096.

[74] Cortes-Canteli M, Mattei L, Richards AT, Norris EH, Strickland S (2015) Fibrin deposited in the Alzheimer's disease brain promotes neuronal degeneration. *Neurobiol Aging* **36**, 608-617.

[75] Cortes-Canteli M, Paul J, Norris EH, Bronstein R, Ahn HJ, Zamolodchikov D, Bhuvanendran S, Fenz KM, Strickland S (2010) Fibrinogen and beta-amyloid association alters thrombosis and fibrinolysis: A possible contributing factor to Alzheimer's disease. *Neuron* **66**, 695-709.

[76] Ryu JK, McLarnon JG (2009) A leaky blood-brain barrier, fibrinogen infiltration and microglial reactivity in inflamed Alzheimer's disease brain. *J Cell Mol Med* **13**, 2911-2925.

[77] Davalos D, Ryu JK, Merlini M, Baeten KM, Le Moan N, Petersen MA, Deerinck TJ, Smirnoff DS, Bedard C, Hakozaki H, Gonias Murray S, Ling JB, Lassmann H, Degen JL, Ellisman MH, Akassoglou K (2012) Fibrinogen-induced perivascular microglial clustering is required for the development of axonal damage in neuroinflammation. *Nat Commun* **3**, 1227-1227.

[78] Jenkins DR, Craner MJ, Esiri MM, DeLuca GC (2018) Contribution of fibrinogen to inflammation and neuronal density in human traumatic brain injury. *J Neurotrauma* **35**, 2259-2271.

[79] Ahn HJ, Chen ZL, Zamolodchikov D, Norris EH, Strickland S (2017) Interactions of beta-amyloid peptide with fibrinogen and coagulation factor XII may contribute to Alzheimer's disease. *Curr Opin Hematol* **24**, 427-431.

[80] Kang G, Zhang Y, Liu R, Li R, Kang Q, Zhu X, Yan L, Yu Y, Yu Q (2019) Fibrinogen and kininogen are potential serum protein biomarkers for depressive disorder. *Clin Lab* **65**, doi: 10.7754/Clin.Lab.2019.190312

[81] Han Y, Chen W, Song Y, Yuan Y, Li Z, Zhou Y, Liu T, Han D, Mi X, Li M, Wang G, Zhong L, Zhou J, Guo X (2020) Proteomic analysis of preoperative CSF reveals risk biomarkers of postoperative delirium. *Front Psychiatry* **11**, 170.

[82] Baker SK, Chen ZL, Norris EH, Revenko AS, MacLeod AR, Strickland S (2018) Blood-derived plasminogen drives brain inflammation and plaque deposition in a mouse model of Alzheimer's disease. *Proc Natl Acad Sci U S A* **115**, E9687-e9696.

[83] Baker SK, Chen Z-L, Norris EH, Strickland S (2019) Plasminogen mediates communication between the peripheral and central immune systems during systemic immune challenge with lipopolysaccharide. *J Neuroinflammation* **16**, 172.

[84] Terrando N, Park JJ, Devinney M, Chan C, Cooter M, Avasarala P, Mathew JP, Quinones QJ, Maddipati KR, Berger M (2021) Immunomodulatory lipid mediator profiling of cerebrospinal fluid following surgery in older adults. *Sci Rep* **11**, 3047.